Journal of the Civil Engineering Forum, May 2022, 8(2):139-146
DOI 10.22146/jcef.3797
Available Online at https://jurnal.ugm.ac.id/jcef/issue/archive

Development of a Density Gauge for Measuring Water and Mud Density based on a Radioactive Technique

Aloysius Bagyo Widagdo*
National Research and Innovation Agency, INDONESIA
*Corresponding author: aloy001@brin.go.id

SUBMITTED 11 October 2021 **REVISED** 2 December 2021 **ACCEPTED** 7 January 2022

ABSTRACT The density or concentration of mud is one of the key variables in studying cohesive sediments, due to being accumulated through settlement and consolidation, as well as resuspended through erosion. This indicates that the proper measurement of sediment density is important. Therefore, this study aims to evaluate the accuracy of density measurement by using the gamma-ray attenuatioan method as a non-intrusive technique. For Compton Scattering, gamma-ray attenuation was effectively independent of mineralogy, subsequently depending on only the electron density of material, which is directly related to the bulk density of the mixture. Based on the results, the advantages of utilizing the nucleonic density gauge indicated that the technique was non-intrusive and very flexible for many experimental arrangements, as well as the high accuracy of measurements with errors less than 1%.

KEYWORDS Density; Cohesive sediment; Nucleonic gauge; Non-intrusive; High accuracy

1 INTRODUCTION

The experimental methods for determining the density of sediments are generally categorized as (i) sampling, and (ii) in situ direct measurements. This sampling method involves weighing an accurately known volume of samples obtained through a siphon, pipette or other devices. Meanwhile, the in-situ direct technique involves optical or acoustic instruments, which are non-intrusive although requires calibration to produce absolute sediment concentrations. These methods have presently been applied in studying suspended layers with materials coarser than mud (i.e., silt and sand). In several previous decades, the initiation of applying the principle of gamma-ray attenuation was conducted in measuring the bulk density of cores and sediment samples. This method was used for the in-situ measurement of bulk sea bottom sediment density (Preiss, 1968*a*,*b*; Rose and Ronsy, 1971; Krishnamurthy et al., 1973; Gerland and Villinger, 1995; Blum, 1997), where vertical distribution was determined at distances between 2-5 cm, with the accuracy of +1%. It was also applied for measuring the spatial variability of soil bulk density (Pires et al., 2009). Furthermore, the gamma-ray attenuation method was used as a proof-of-concept for non-intrusive and undisturbed measurement of sediment infiltration masses. This led to a good accuracy with a deviation of less than 5% (Mayar et al., 2020).

Based on this present study, the development and evaluation of a nucleonic density gauge are required, as a non-intrusive method for the accurate concentration measurements of mud profiles. This density gauge is a device for measuring the attenuation of a collimated gamma-ray beam after passing through a test material, e.g., the sediment-water mixture. The gauge utilized in this application uses a 111 MBq source, which emits a narrow collimated beam of gamma-rays at 662 keV. At this energy level, attenuation is found to occur by the Compton scattering of the incident gamma-rays from the collimated beam. This method is non-intrusive and has the additional important advantage that the calibration factor (i.e., the ratio between the measured gamma-ray attenuation and the calculations from the published coefficients of the kaolin and water com-

ponents) is close to unity. The nucleonic density gauge method was also evaluated for environmental engineering applications, by studying the profile of kaolin-water mixtures in controlled laboratory experiments. In addition, the cohesive sediment model for the experiments was kaolin (dry density (ρ_s) of 2610 g/L and d_{50} of 1.08 µm), with density ranging from a very dense mud in the bed to a low water surface concentration.

2 METHODOLOGY

2.1 Theory of Gamma attenuation

The method relied on the interaction of the medium-energy gamma-rays (0.1 – 5 MeV) with the geological materials, specifically through Compton scattering (Preiss, 1968*a*), where gamma-ray attenuation was effectively independent of mineralogy. It also depended only on the electron density of the material, which is directly related to the bulk mass of the mixture. When a mono-energetic narrow beam of gamma-rays (in this case 662 keV from a Cs-137 source) passes through a material of thickness d, in the Compton scattering range with an incident flux I_0, the transmitted flux I is provided in Equation 1 as follows:

$$I = I_0 \exp\left[-\mu\rho_b \mathrm{d}\right] \tag{1}$$

where μ, ρ_b, and d = the mass attenuation coefficient, bulk density, and thickness of the material, respectively.

As gamma-ray passes through four different materials in the experimental set-up, i.e., air, plexiglasses, water, and kaolin, the intensity of the beam at the detector is expressed in Equation 2 as follows:

$$\begin{aligned} I =& I_0.exp -[\mu_{ga}\rho_a d_a \\ &+ \mu_{gg}\rho_g d_g + \mu_{gw}\rho_w d_w \\ &+ \mu_{gs}\rho_s d_s] \end{aligned} \tag{2}$$

where I = detected radiation intensity (cps = counts per second), I_0 = initial radiation intensity (cps), μ_{ga}, μ_{gg}, μ_{gw}, μ_{gs} = mass attenuation coefficients for air, plexiglass, water, and sediment (cm^2/g), respectively, ρ_a, ρ_g, ρ_w, ρ_s = the densities of air, plexiglass, water, and sediment (g/cm^3), respectively, d_a, d_g, d_w, d_s = the path length of the beam through the air, plexiglass, water, and sediment (cm), respectively.

For the reference (or calibration) configuration with pure water in the plexiglass containment vessel, the beam path length for the sediment was occupied by the fluid and radiation intensity, I_{calib}, as shown in Equation 3:

$$\begin{aligned} I_{calib} =& I_0.exp -[\mu_{ga}\rho_a d_a \\ &+ \mu_{gg}\rho_g d_g + \mu_{gw}\rho_w(d_w + d_s)] \end{aligned} \tag{3}$$

By substituting Equation 3 into 2, Equation 4 is provided:

$$\frac{I}{I_{calib}} = exp -[(\mu_{gs}\rho_s - \mu_{gw}\rho_w)d_s] \tag{4}$$

Using the definitions of ρ_w, ρ_s, ρs_w, the rearrangement of Equation 4 allowed the density of the sediment-water mixture to be determined from the measured intensity in Equation 5 as follows:

$$\rho_{sw} = \rho_w - \ln\left(\frac{I}{I_{calib}}\right)\left[\frac{(\rho_s - \rho_w)}{(\mu_{gs}\rho_s - \mu_{gw}\rho_w)d_{sw}}\right] \tag{5}$$

2.2 Statistical uncertainties

The parameters involved in the measurement of radioactivity had two major components, namely the error and statistical uncertainties, which were due to the experimental configuration and random process of the radioactive decay. The measurement error is defined as the difference between the true and measured values, with the magnitude being difficult to quantify. This was due to the true value being unknown. Meanwhile, statistical analysis should be applied while processing the measured data. This indicated that the mean was adopted as the best estimate of the true value. It was also defined as the mean value plus/minus a standard error (Sn), which accuracy for normal distribution is shown in Equation 6 as follows:

$$S_n = \frac{\sigma}{\sqrt{n}} \tag{6}$$

Table 1. Properties of the samples for calibration of the nucleonic gauge AM214

No	Test Code	ρ_{sw} (g/L)	C_M (g/L)	M_R (%)
1	Cal-water	998.00	0.00	
2	Cal-1125	1121.58	200.09	460.53
3	Cal-1250	1249.96	407.95	206.40
4	Cal-1350	1347.68	566.17	138.04
5	Cal-1450	1452.76	736.31	97.30

An interval for the measured mean intensity was also determined based on a 95% confidence level. According to the normal curve probability density function for the 95% level, the confidence interval provided a 1.96 standard error.

2.3 Experimental setup

To prepare sediment samples with different and known concentrations, commercial kaolin was mixed with Sydney tap water (density of 998 g/L) in specific proportions. This indicated that 5 samples were prepared, with 1 and 4 observed for water and kaolin-water mixtures of different densities, respectively. The details of these samples are presented in Table 1. In determining the density ($_{sw}$), the samples were precisely characterized by their mass concentration (C_M) and water content (M_R).

The experiment was conducted using the plexiglass containment vessel, which container had external and internal dimensions of 400 x 135 x 33 mm and 350 x 117 x 24 mm, respectively. This container was then placed into the space between gamma-ray source and detector. The detail of the experimental setup is shown in Figure 1.

3 STUDY RESULTS

Equation 6 showed that the standard error in the measured mean radiation intensity reduced to zero, with the count time observed at infinity. This indicated that the error was reduced by increasing the radioactive source strength, although it was not always practical. In addition, an acceptable standard error and tolerable count time should practically be decided for each experimental setup. To determine the contribution of the experimental setup to the mean standard error, very long count times were conducted for the negligible performance of the random radioactive decay process. Based on the relatively high measured gamma intensity (> 1000 cps), the results showed that a 20-minute count time reduced the contribution of the decay statistical error to < 0.05%. Therefore, approximately 1200 s counts were experimentally obtained for each sample (total counting time 20 min), with the distribution analyzed to derive the average value, standard deviation, and bounds for the 95% confidence level. The results are summarized in Table 2.

Based on Tables 1 and 2, as well as Equation 5, the theoretical relationship between the density of the kaolin-water mixture and the mean radiation intensity was determined as follows:

ρ_w = 998 g/L = 0.998 g/cm^3 (Table 1)

ρ_s = 2610 g/L = 2.61 g/cm^3

I_{calib} = 1626.25 cps (the radiation intensity of gamma-ray passing through water in the system, calculated based on Equation 4)

μ_{gw} = 0.0857 cm$^{\text{w}}$/g (theoretically known; Airey, 1997)

μ_{gs} = 0.075 cm^2/g (theoretically known; Airey, 1997)

d_{sw} = 11.7 cm (internal length of the slim container, Figure 1)

By applying Equation 5 and using the variable value above, the density of kaolin-water mixture ρ_{sw} was calculated as follows:
ρ_{sw} = -1.250009 ln($\bar{I}$)+10.24061 (g/cm)^3
or in the unit of (g/L), the theoretical result was written as:

$$\rho_{\text{sw}} = -1250.01ln(\bar{I}) + 10240.61(g/L) \quad (7)$$

where $\bar{I}$ and ρ_{sw} = the mean gamma-ray intensity (cps) at the detector and density of the mixture (g/L), respectively. Based on Figure 2, the theoretical relationship was shown in blue colour, with the observation of a very good correlation with the measured values (R^2 = 0.9995). In addition, the fitted calibration curve for the 10 data points was observed (Figure 2), providing a slightly better correlation as follows:

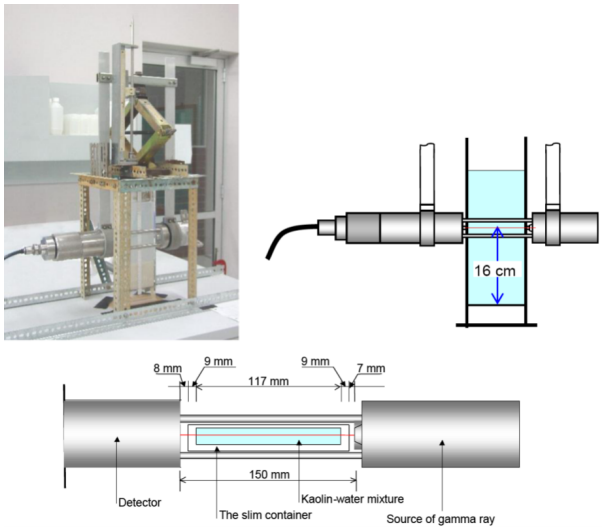

Figure 1 The experimental setup of calibration for the gauge model AM214. The container with an inner dimension of 350 x 117 x 24 mm was placed between gamma-ray source and detector. The position of the beam of gamma-ray was 16 cm from the bottom

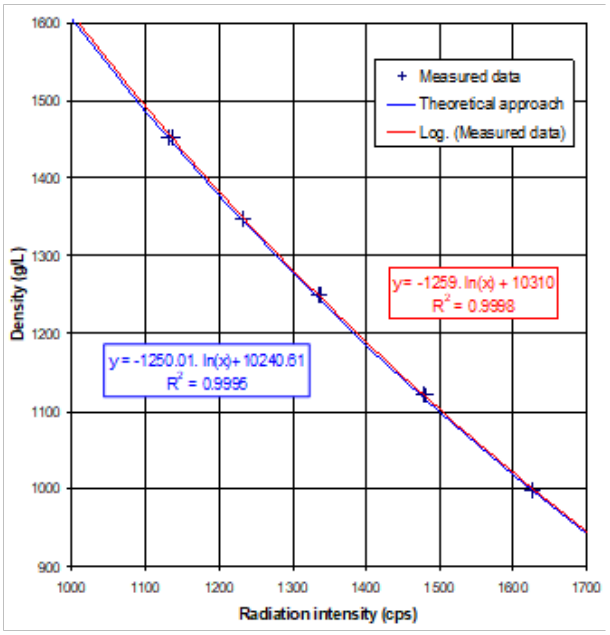

Figure 2 The relation between density ρ_{sw} and measured mean radiation intensity $\bar{I}$ for the nucleonic gauge AM214, as prepared in Tables 1 and 2. Logarithmic regression on the 10 data points and theoretical relation (using Equation 7) are compared

Table 2. Mean intensity, standard deviation, and standard error of the samples using the nucleonic density gauge AM214

Test Code	Mean Intensity, (cps)	Standard deviation, *s* (cps)	Standard error, *Sn* (cps)	Error at confidence level 95% (cps)	(%)
Cal-water #1	1625.35	38.50	1.11	2.18	0.134
#2	1627.15	37.23	1.08	2.11	0.130
Cal-1125 #1	1479.92	37.30	1.08	2.11	0.143
#2	1481.49	36.87	1.06	2.09	0.141
Cal-1250 #1	1337.88	35.64	1.03	2.02	0.151
#2	1336.26	35.36	1.02	2.00	0.150
Cal-1350 #1	1233.63	34.62	1.00	1.96	0.159
#2	1233.93	33.90	0.98	1.92	0.155
Cal-1450 #1	1133.69	31.88	0.92	1.80	0.159
#2	1135.53	32.04	0.93	1.81	0.160

$$\rho_{\text{sw}} = -1259ln(\bar{I})+) + 10310(g/L) \qquad R^2 = 0.9998 \tag{8}$$

Although Equation 8 was slightly better than the theoretical relationship based on logarithmic regression, the data in Equation 7 still contained some errors/discrepancies recognized as the 95% confident interval. Therefore, this relationship was adopted to determine the density of the sediment-water mixture, for subsequent experiments.

4 STATISTICAL ASSESSMENT

The chi-squared (χ^2) test was applied to show the functional accuracy of gamma-ray counting measurement, with the adopted parameters and equations shown as follows:
The chi-squared statistic value:

$$\chi^2 = \frac{\sum_{i=1}^{n}(x_i - \bar{x})^2}{\bar{x}} \tag{9}$$

The standard deviation of the chi-squared distribution:

$$\sigma = \sqrt{\bar{x}} \tag{10}$$

Table 3. Results of analysis of the counting data using the chi-square (χ^2) test.

Test Code	Number of data, n	$\chi^2$0.975	χ^2	$\chi^2$0.025	Remark
Cal-water #1	240	198.98	207.06	284.81	not reject the null hypothesis
#2	100	73.35	74.06	128.43	not reject the null hypothesis
Cal-1125 #1	1200	1104.93	1126.18	1296.86	not reject the null hypothesis
#2	1100	1009.02	1009.32	1192.77	not reject the null hypothesis
Cal-1250 #1	1200	1104.93	1132.67	1296.86	not reject the null hypothesis
#2	1200	1104.93	1122.25	1296.86	not reject the null hypothesis
Cal-1350 #1	1200	1104.93	1165.28	1296.86	not reject the null hypothesis
#2	1200	1104.93	1115.87	1296.86	not reject the null hypothesis
Cal-1450 #1	1100	1009.02	1011.03	1192.77	not reject the null hypothesis
#2	1000	914.25	916.22	1089.53	not reject the null hypothesis

The observed standard deviation:

$$s = \sqrt{\frac{\sum_{i=1}^{n}(x_i - \bar{x})}{n-1}} \quad (11)$$

where $\overline{x}$ and n = the average value and number of the counts, respectively.
The null hypothesis = H_0:$\mu = s$
The alternative hyphothesis is: H_1:$\mu \neq s$ The results showed that the null hypothesis was rejected when:

$$\chi^2 > \chi^2_{n-1,\alpha/2} or \chi^2 < \chi^2_{n-1,1-\alpha/2} \quad (12)$$

where α = a number between 0 and 1, which is determined from the level of confidence used in this data analysis. Based on the 95% confidence level, α = 0.05.

The results of the chi-squared test are shown in Table 3, where the values of χ^2 were observed in the external rejection region, as indicated in Equation 12. Therefore, the null hypothesis was accepted, indicating that the counter was accurately functioning.

A frequency distribution assessment was also applied for the counting data, to identify the information distribution. Moreover, a frequency histogram was used and compared with the normal distribution, as each sample are presented in Figures 3-7. The graphs subsequently indicated that the counting data distribution was close to the normal type, where significant correlations were observed in all patterns. However, minor skewness was found in the counting data. This indicated that the statistical equations of normal distribution were appropriate for the application of gamma-ray counting data in this study, where a confident level of 95% was adopted.

5 DISCUSSION

Based on the settlement and consolidation of the kaolin-water mixture over time, the density profile continually changed in the measurement period. This indicated that the measurement durations of the radiation intensity should be very short at specifically selected points in the vertical profile (specifically those with low sediment concentration), to avoid introducing further unacceptable errors into the experiment. Also, the optimization of the gamma-ray attenuation method application (related to radiation statistical errors) should be conducted by adjusting the measurement time (Mayar et al., 2019). To determine the relationship between the confidence interval and the time duration of the measurements, the 20-minute data was subsequently reduced for a specific time length. This was further applicable in determining the shortest acceptable measurement period. In this study, eight new data were created from the original 20-minute information at 30, 60, 90, 120, 180, 360, 600, and 1200 s, respectively. All the new data were also observed to begin at the same time as the original one. Based on Figure 8, the confidence interval is observed as a function of the measurement duration for each of the 5 different density samples (Table 1).

This indicated that a decrease in the confidence interval (%) was observed with an increased measurement time. To optimize the measurement of density within an acceptable standard error, the choice of a tolerable assessment time should be balanced with the temporal variability of the system. For example, captured rapid data improved the time local representation of the measurement,

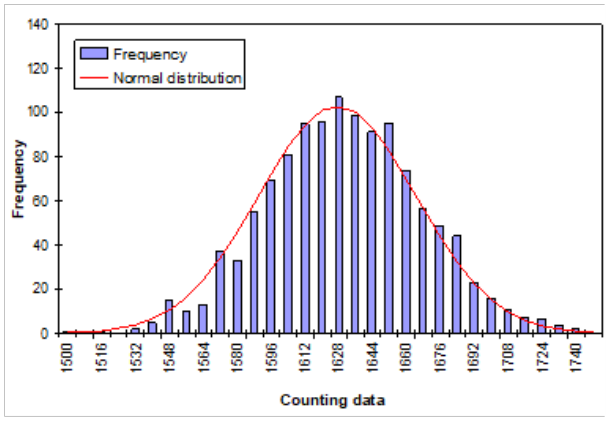

Figure 3 Distribution of counting data of sample Cal-water 2 and its comparison with the Normal Distribution

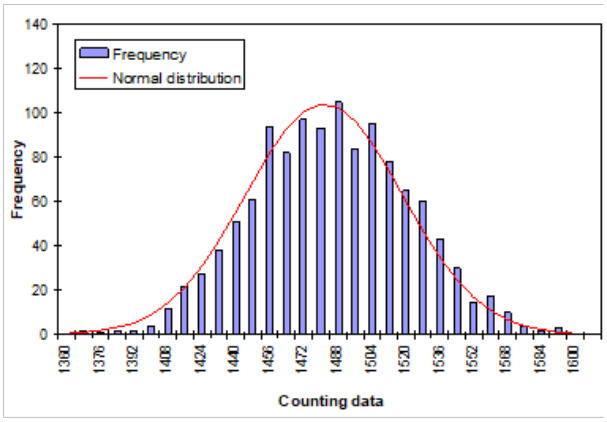

Figure 4 Distribution of counting data of sample Cal-1125 2 and its comparison with the Normal Distribution

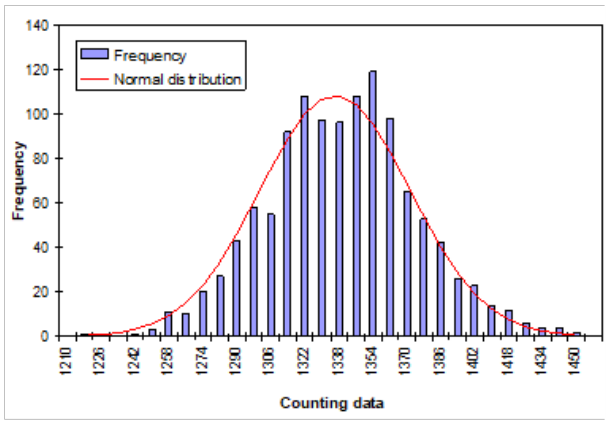

Figure 5 Distribution of counting data of sample Cal-1250 2 and its comparison with the Normal Distribution

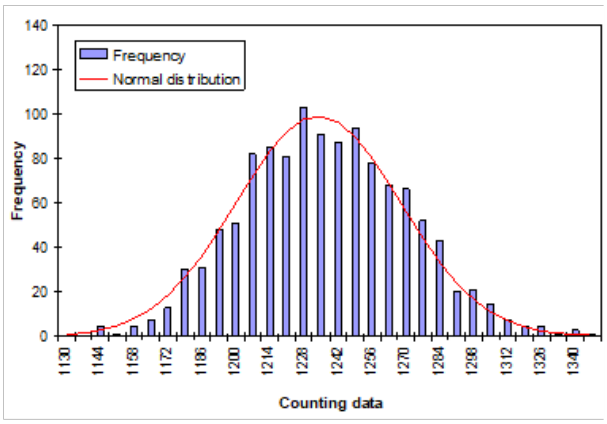

Figure 6 Distribution of counting data of sample Cal-1350 2 and its comparison with the Normal Distribution

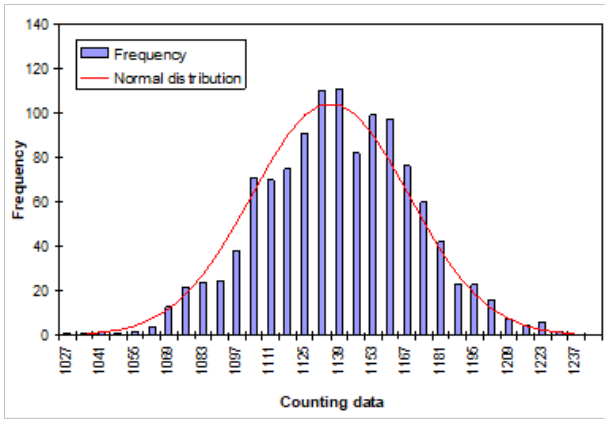

Figure 7 Distribution of counting data of sample Cal-1450 2 and its comparison with the Normal Distribution

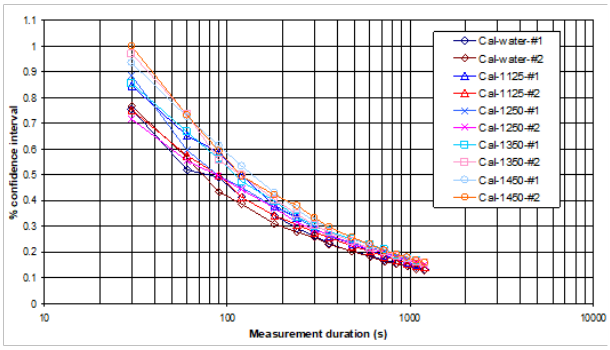

Figure 8 The % confidence interval of the measured mean radiation intensity as a function of measurement duration

leading to an increase in the confidence interval (%).

6 CONCLUSIONS AND RECOMMENDATIONS

To measure the density profiles of kaolin-water mixtures in the laboratory, the results of the nucleonic density gauge application are summarized as follows:

(a) Based on substituting the data in Table 2 into the graph in Fig. 2, a very good relationship was observed with the theoretical equation (Eq. 7), leading to a correlation coefficient of 0.9995. This indicated that Eq. 7 was suitable for calculating the sample density.
(b) Through the assessment of the counting data using the Chi-square test, the χ^2 values were observed at the external rejection area, indicating that the counter was accurately working.
(c) By comparing the counting data with the normal distribution, all the distributed patterns were closely related, with a minor skewness being observed. This indicated that the data were analyzed with the statistical equation of a normal distribution, through the adoption of a 95
(d) Based on Figure 8, the maximum error captured in this experiment was 1
(e) Optimizing the time duration of the radiation intensity measurements was also a necessary and important step while using nucleonic density gauges. Based on statistics, increasing measurement times improved the accuracy of the density produced.
(f) Within its range of applications, the technique was non-intrusive and very flexible. In many study arrangements, counting statistics were the only significant component of the random experimental error.

DISCLAIMER

The authors declare no conflict of interest.

AVAILABILITY OF DATA AND MATERIALS

All data are available from the author.

ACKNOWLEDGMENTS

This experiment was conducted at the Australian Nuclear Science and Technology Organization (ANSTO) in 2004. The author would like to thank distinguished members of the ANSTO, Dr. Suzanne Hollins, Dr. Cath Hughes, and Dr. Peter Airey for their support, assistance, and guidance in carrying out measurements using the nuclear-based density gauge.

REFERENCES

Blum, P. (1997), 'Physical properties handbook: a guide to the shipboard measurement of physical properties of deep-sea cores'.

Gerland, S. and Villinger, H. (1995), 'Nondestructive density determination on marine sediment cores from gamma-ray attenuation measurements', *Geo-Marine Letters* **15**(2), 111–118.

Krishnamurthy, K., Rao, S. and Rajagopalan, R. (1973), 'Nucleonic sediment concentration gauge comparison of transmission and scattering modes', *The International Journal of Applied Radiation and Isotopes* **24**(10), 579–583.

Mayar, M., Schmid, G., Wieprecht, S. and Noack, M. (2019), 'Optimizing vertical profile measurements setup of gamma ray attenuation', *Radiation Physics and Chemistry* **164**, 108376.

Mayar, M., Schmid, G., Wieprecht, S. and Noack, M. (2020), 'Proof-of-concept for nonintrusive and undisturbed measurement of sediment infiltration masses using gamma-ray attenuation', *Journal of Hydraulic Engineering* **146**(5), 04020032.

Pires, L., Rosa, J., Pereira, A., Arthur, R. and Bacchi, O. (2009), 'Gamma-ray attenuation method as an efficient tool to investigate soil bulk density spatial variability', *Annals of Nuclear Energy* **36**(11-12), 1734–1739.

Preiss, K. (1968*a*), In situ measurement of marine sediment density by gamma radiation., Technical report, Negev Inst. for Arid Zone Research, Beer-Sheva, Israel.

Preiss, K. (1968*b*), Non-destructive laboratory measurement of marine sediment density in a core barrel using gamma radiation, *in* 'Deep Sea Research and Oceanographic Abstracts', Vol. 15, Elsevier, pp. 401–407.

Rose, V. C. and Ronsy, J. R. (1971), A nuclear gage for in-place measurement of sediment density, *in* 'Offshore Technology Conference', OnePetro.